

Part 1

**EXTRASOLAR PLANETARY
SYSTEMS**

Resonances and stability of extra-solar planetary systems

C. Beaugé¹, N. Callegari Jr.², S. Ferraz-Mello³ and
T.A. Michtchenko³

¹ Observatorio Astronómico, Universidad Nacional de Córdoba, Laprida 854, (X5000BGR) Córdoba, Argentina (beaugé@oac.uncor.edu)

² Departamento de Matemática, Universidade Federal de São Carlos, São Carlos, Brasil

³ Instituto de Astronomia, Geofísica e Ciências Atmosféricas, Universidade de São Paulo, Cidade Univesitária, 05508-900 São Paulo, Brasil (sylvio@usp.br)

Abstract. This paper reviews recent results on the dynamics of multiple-planet extra-solar systems, including main sequence stars and the pulsar PSR B1257+12 and, comparatively, our own Solar System. Taking into account the degree of gravitational interaction of the planets, the known planetary systems may be separated into four main groups: (Ia) Planets in Mean-motion resonance (Ib) Low-eccentricity near-resonant pairs; (II) Non-resonant planets with a significant secular dynamics; and (III) Weakly interacting planet pairs. Different analytical and numerical tools can help to understand the structure of the phase space, to identify stability mechanisms and to categorize different types of motions in the cases of more significant dynamical interaction. The origin of resonant configurations is discussed in the light of the hypothesis of planetary migration.

Keywords. Exoplanets, stability, resonances

1. Introduction

Currently 12 systems with 2 or more planets around Main Sequence stars are known (see Schneider, 2004) and others are to be announced soon. Twelve of them are shown in Table 1. When the ratio of orbital periods in each planet pair is plotted (fig. 1), we see a more or less continuous distribution (at least in a logarithmic scale) between two extreme cases: In the lower end, we have planet pairs with $P_2/P_1 \approx 2$ and at the upper end, $P_2/P_1 > 300$. We may distinguish, tentatively, three different classes (one of which includes two sub-classes).

Class Ia. Planets in Resonant Orbits (MMR)

We put in Class I those planets at the lower end of the distribution shown in figure 1 with large masses and eccentricities and orbiting in relatively small orbits. These planets are liable to strong gravitational interaction and are significantly perturbed over orbital timescales. They are unable to remain stable if not tied by a mean-motions resonance (MMR). They are among the more interesting extra-solar systems for Celestial Mechanics studies.

The first two pairs are the two well-known pairs in 2:1 mean-motion resonance: HD 82943 and GJ 876 (= Gliese 876). The next two pairs appear in fig. 1 with open circles because of doubts concerning one of the planets in the pair. They are 47 Uma and the planets b,c of 55 Cnc. In these 2 pairs, the outer planet cannot yet be considered as confirmed, as there is no consensus among the observers about their existence (Naef

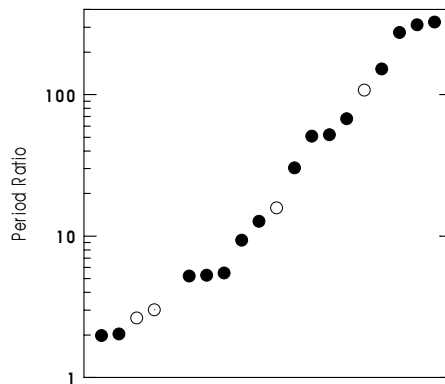


Figure 1. Ratio of the orbital periods of pairs of planets in motion around a main sequence star (see text for details). Open circles indicate pairs for which the existence of one of the components is still under discussion. The abscissas (not shown) are just sequence numbers of the pairs arranged in increasing order.

et al. 2004). If the existence of 55 Cnc c and the resonance is confirmed, this planet pair will be added to the two known resonant pairs to form a set of examples whose study may contribute to our understanding of the physics underneath the capture of exoplanets into resonance. A recent paper considers that the planetary hypothesis for the 44-day oscillations in the radial velocity is more likely because this star is a very inactive star (McArthur *et al.* 2004).

The planets of 47 UMa have large orbits and small eccentricities and, perhaps, may remain stable even in non-resonant orbits, in which case this system would rather be considered in Class Ib.

Class Ib. Low-eccentricity Near-resonant pairs

This is a special class including systems with low-eccentricity planets in successive pairs, with small period ratio, but with circumstances making the gravitational interaction between the planets less important. We put in this class the planets pairs of the pulsar PSR B1257+12. We may also include here the planets of the two sub-systems of the Solar System. In the planetary system of the pulsar PSR B1257+12 (see Table 2), as well as in the inner Solar System, the orbits are relatively close one to another, but the masses are relatively small. In the outer Solar System the masses are larger, but the distances between the planets is always large allowing this system to show long-term stability notwithstanding the fact that the planets have low period ratios.

The most conspicuous characteristic, here, is the presence of a large number of pairs in near resonance. The most conspicuous examples are the pair Jupiter-Saturn with a period ratio ~ 2.5 (5:2 MMR) (see Michtchenko and Ferraz-Mello, 2001b) and the two outer planets of the pulsar PSR B1257 +12 with period ratio ~ 1.5 (3:2 MMR). The closeness of the pulsar outer planets to commensurability produces perturbations large enough to be observed from Earth thus allowing the very existence of the planets to be confirmed in a few years of continuous observations (Rasio *et al.* (1992); Malhotra *et al.* (1992)).

Among the extra-solar systems, the low-eccentricity planets of 47UMa are possibly to be included in this class. The current orbits are near the resonance 8/3, but new observations are necessary to confirm the data of this system.

Table 1. Extra-solar Planetary Systems with 2 or more planets †

Star/ spectrum	planet	mass \times sin i (m_{Jup})	period (days)	period ratio	semi-major axis (AU)	eccentricity
HD 82943 ⁽¹⁾	c	1.7	219.5	1.99	0.75	0.39
G0	b	1.8	436.2		1.18	0.15
GJ 876 ⁽²⁾	c	0.56	30.12	2.03	0.13	0.27
M4 V	b	1.89	61.02		0.21	0.10
47 UMa ⁽²⁾	b	2.9	1079.2	2.64	2.1	0.05
G0 V	c (?)	1.1	2845.0		4.0	0
55 Cnc ⁽³⁾	e	0.045	2.81	5.2	0.038	0.2
(= ρ^1 Cnc)	b	0.78	14.7		2.99	0.115
G8 V	c (?)	0.22	43.9	103	0.24	0.44
	d	3.91	4517		5.26	0.3
μ Ara ⁽⁴⁾	d	0.044	9.55	67.5	0.09	–
(=HD 160691)	b	1.67	645		4.63	1.50
G3 IV-V	c	3.1	2986		4.2	0.6
ν And ⁽²⁾	b	0.64	4.617	52.2	0.058	0.01
F8 V	c	1.79	241.16		5.29	0.805
	d	3.53	1276.1		2.543	0.25
HD 12661 ⁽²⁾	b	2.30	263.6	5.48	0.823	0.35
G6	c	1.57	1444.5		2.557	0.20
HD 169830 ⁽⁵⁾	b	2.88	225.62	9.32	0.81	0.31
F8 V	c	4.04	2102		3.6	0.33
HD 37124 ⁽²⁾	b	0.86	153.3	12.7	0.543	0.1
G4 IV-V	c	1.0	1942		2.952	0.4
HD 168443 ⁽²⁾	b	7.64	58.1	30.5	0.295	0.53
G5	c	16.96	1770		2.873	0.20
HD 74156 ⁽²⁾	c	1.61	51.6	> 51	0.745	0.65
G0	b	>8.2	>265		>3.82	0.35
HD 38529 ⁽²⁾	b	0.78	14.309	152	0.129	0.29
G4	c	12.7	2174.3		3.68	0.36

† Update: Oct. 2004. ϵ Eri pair is too uncertain and was not included.

⁽¹⁾ Ref: Ferraz-Mello *et al.* (2005).

⁽²⁾ Ref: Fischer *et al.* (2003).

⁽³⁾ Ref: McArthur *et al.* (2004).

⁽⁴⁾ Refs: Santos *et al.* (2004), McCarthy *et al.* (2004).

⁽⁵⁾ Ref: Schneider (2004).

Class II. Non-resonant Planets with a Significant Secular Dynamics

The period ratio of the planet pairs considered in this class lies above 4.5 and is large enough to make very difficult a capture into a MMR. The gravitational interaction between these planets may be strong but the conservation of the angular momentum limits the eccentricity variations, allowing them to remain stable even if not in a MMR. They present long-term variations, primarily described by secular perturbations, large

Table 2. Planetary System of the pulsar PSR B1257+12†

Star	planet	mass (m_{Earth})	period (days)	period ratio	semi-major axis (AU)	eccentricity	inclination (degrees) ‡
B1257 +12	A	0.020‡‡	25.262	2.63	0.19	0.	
	B	4.3	66.5419		0.36		
	C	3.9	98.2114	1.47	0.46	0.0252	47

† Ref: Konacki and Wolszczan (2003). Adopted pulsar mass: $1.4M_{\odot}$

‡ over the tangent plane to the celestial sphere.

‡‡ adopting the inclination $i = 50^{\circ}$

variation of the eccentricities and interesting dynamical effects such as the alignment and anti-alignment of the apsidal lines (see Michtchenko and Malhotra, 2004).

Among the extra-solar planetary systems, the most conspicuous examples in this class are three important systems: the outer planets of μ Ara, HD 12661 and the outer planets of ν And. In all cases, they do not seem to be in MMR or close to one; the outer planets of ν And are paradigms of systems showing apsidal lock due to a non-resonant secular dynamics.

Class III. Weakly interacting Planet Pairs

These are the planets given at the bottom of table 1. One example is HD 38529 where $P_2/P_1 \sim 150$. The outermost and innermost planets of 55 Cnc are such that $P_2/P_1 \sim 1700$ forming the more separated known pair (out of the scale of fig. 1). The large period ratios (> 30) allow these planets to be considered as weakly interacting planets; the mutual gravitational interaction exists, but is less important than in the previous case and the probability of capture in a MMR is negligible. We remind that in many dynamical studies of the outer Solar System, the mass of the inner planets is just added to the mass of the Sun!

Two of the candidates to this category are the planets around HD 168443 and HD 74156. However, these systems have some very massive planets and the use of hierarchical models to study these pairs should be preceded of specific analysis.

2. Chaos

Chaos is a common feature in systems with many degrees of freedom. In systems with several planets, the neighborhood of the planets is filled by MMR. In the considered low-eccentricity systems, the near resonant motion of neighboring planets gives rise to a dense set of three-planet resonances, which occur when the periods corresponding to two two-planet MMR form critical linear combinations. Jupiter and Saturn lie very close to the 5:2 MMR, Uranus is confined between the domains of the overlap of the 7:1 MMR with Jupiter and the 2:1 MMR with Neptune in one side, and the 3:1 MMR with Saturn in the other; finally, Neptune is close to the 2:1 MMR with Uranus.

The resonant structure of these systems may be known through dynamical maps constructed in the neighborhood of the actual planets (Michtchenko and Ferraz-Mello, 2001a). In these maps, the initial values of the semi-major axis and eccentricity of one planet are uniformly chosen on a rectangular grid covering the vicinity of its actual position, while the initial positions of the other planets are fixed to the actual values at the chosen epoch. The short-term oscillations (of the order of the orbital periods) are eliminated by employing a low-pass filtering procedure *on-line* with the numerical integration and the resulting semi-major axes are used to construct the maps. The spectral

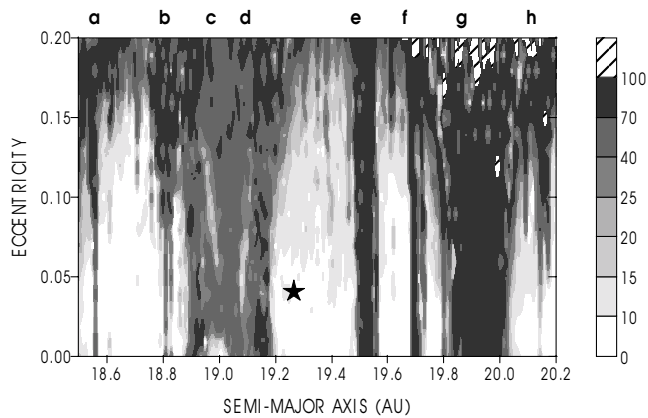


Figure 2. Dynamical map of the neighborhood of Uranus. The main apparent MMR are indicated on top of the figure by the letters a-h and identified in table 3. The star shows the current position of Uranus. (Taken from Michtchenko and Ferraz-Mello, 2001a.)

Table 3. Main MMR in Uranus' neighborhood

Position (fig. 2)	MMR†	Remarks (beat)
a	J-S-4U	beat of J-7U and S-3U
b	3J-10S+7U	beat of 2(2J-5S) and J-7U
c	U-2N	
d	J-7U	
e	2J-6S+3U	beat of 2J-5S and S-3U
f	2J-6S+3U	beat of 2J-5S and 2(S-3U)
g	S-3U	
h	2J-3S+6U	beat of 2J-5S and -2(S-3U)

† $k_1J \pm k_2S \pm k_3U \pm k_4N$ means the MMR $k_1n_J \pm k_2n_S \pm k_3n_U \pm k_4n_N \approx 0$

number N presented in the maps is defined as the number of spectral peaks above 5% of the largest peak. The counting is stopped at $N = 100$. Regular orbits are identified with small values of N , while large numerical values correspond to increasingly chaotic trajectories.

Uranus's neighborhood

We present here the dynamical map of the neighborhood of Uranus (figure 2). This neighborhood is dominated by the 3:1 resonance with Saturn (S-3U) and the 2:1 resonance with Neptune (U-2N), one on each side of the actual position of Uranus. There are also several narrow bands of chaotic motion associated with three-planet MMR (see Table 3). The small hatched domains in figure 2 are those in which collisions (i.e. disrupting close approaches) occur in the time span of the numerical integration (50 Myr).

The neighborhood of the outer pulsar planet

The dynamics of the neighborhood of the pulsar planets is not so complex as the neighborhood of the outer Solar System planets. The dynamical map constructed with minimal masses ($\sin i = 1$) is shown in fig. 3. This neighborhood is dominated by the resonance 2B-3C with narrow bands due to several higher-order resonances (indicated above the top axis of fig. 3).

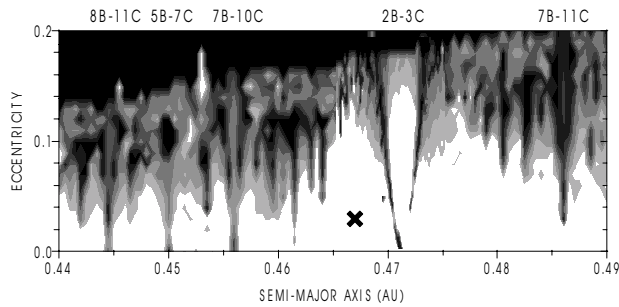


Figure 3. Dynamical map of the neighborhood of PSR B1257+12 planet C. The main apparent MMR are indicated on top of the figure. The cross shows the position of planet C. Same gray scale as fig 2. (Taken from Ferraz-Mello and Michtchenko, 2003.)

3. Dynamics of a MMR and its Neighborhood

We summarize in this section some results of the study of the low-eccentricity dynamics of the 2:1 MMR by Callegari *et al.* (2004) showing how the dynamics of a system of 2 planets evolves when it passes from outside to inside the MMR.

Fig. 4 shows three surfaces of section of the planetary motion defined by the sectioning condition $\theta_1 = 2\lambda_2 - \lambda_1 - \varpi_1 = 0$ and represented on the plane $(x = e_1 \cos \Delta\varpi, y = e_1 \sin \Delta\varpi)$ with $\Delta\varpi = \varpi_1 - \varpi_2$, for three different energy levels[†].

At the right of each surface of section are shown the corresponding dynamic power spectra of the solutions, parameterized by the value of x corresponding to $y = 0$. The points marked in these plots are the points where the frequency in the power spectrum is higher than a given level above noise level. The ordinates are the frequencies (in yr^{-1}). In dynamic power spectra, the lines have the same behavior found in frequency map analysis: frequencies remain almost constant inside resonance islands, have vertical displacements when crossing a saddle point and become erratic when a chaotic layer is reached (Laskar, 1993).

At the lower energy level (top panels in fig. 4), the system is outside the 2:1 MMR; its dynamics is dominated by secular interactions and characterized by two secular modes of motion known from the linear secular theories (see Pauwels 1983). There are two periodic solutions: one at $\Delta\varpi = 0$ and another at $\Delta\varpi = \pi$. In the surfaces of section, these solutions appear as fixed points. These two periodic orbits and the domains around them are indicated as Mode I and Mode II, respectively. The Mode I of motion is located on the right-hand side of the section while Mode II is located on the left-hand side. The curves around the fixed points are quasi-periodic solutions.

Around Mode I, the angle $\Delta\varpi$ oscillates about 0, while around Mode II, $\Delta\varpi$ oscillates about π ; in both cases the eccentricity of the planets vary regularly around the eccentricity value of the periodic orbit. Between the two cases, the angle $\Delta\varpi = \varpi_1 - \varpi_2$ is in *direct* circulation. It can be shown that, in this near resonance zone, the critical angles

$$\begin{aligned}\theta_1 &= 2\lambda_2 - \lambda_1 - \varpi_1 \\ \theta_2 &= 2\lambda_2 - \lambda_1 - \varpi_2\end{aligned}$$

are in circulation. No infinite-period separatrix exist between the solutions around Mode I and Mode II and the quasi-periodic solutions shown in the surface of section form one continuous family. This fact is clearly seen in the corresponding dynamic power spectrum

[†] The subscripts 1 and 2 represent Uranus and Neptune, respectively.

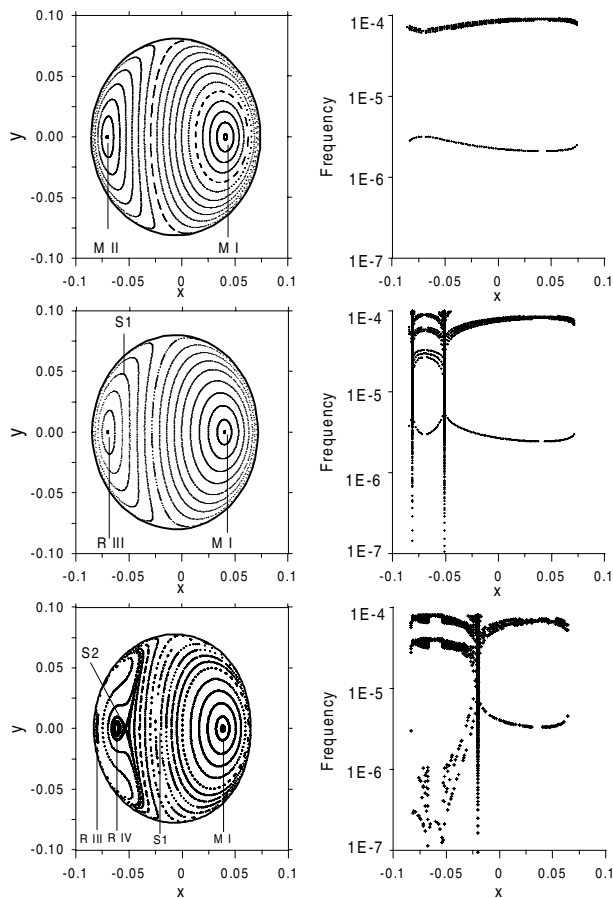


Figure 4. *Left:* Surfaces of Section of the averaged low-eccentricity planetary system in the neighborhood of the 2:1 resonance for three energy levels. Axes $x = e_1 \cos \Delta\varpi$, $y = e_1 \sin \Delta\varpi$. *Right:* Dynamic power spectrum of the solutions parameterized by the value of x corresponding to $y = 0$. Frequencies in yr^{-1} . The planets have the same masses as Uranus and Neptune. (Taken from Callegari *et al.* 2004).

where only two fundamental frequencies and a few harmonics appear. The lower line (at $\sim 3 \times 10^{-6} \text{ year}^{-1}$) corresponds to the proper frequency associated with the angle $\Delta\varpi$. We can see that the line shows a discontinuity near the fixed points, indicating that the amplitude associated to the secular frequency tend to zero at those points. The secular period is $\sim 400,000$ years in the center of Mode I and $\sim 300,000$ years in the center of Mode II. The upper line (at $\sim 10^{-4} \text{ year}^{-1}$) corresponds to the second fundamental frequency, which is associated with the circulation of the critical angles (transversal to the surface of section).

At the next energy level (middle panels in fig. 4), the resonance 2/1 is already visible. The surface of section seems similar to the previous one, but the dynamic power spectrum shows that an important difference exists. The two vertical broad lines seen in the dynamic power spectrum, at the abscissas corresponding to the curve labeled S1 in the surface of section, indicate that S1 is indeed a separatrix (even if it does not show any visible feature in the surface of section). The domain inside S1 (called RIII by Callegari

et al.) is a resonant regime of motion in which the critical angles θ_1 and θ_2 oscillate (librate) about 0 and π , respectively. Their difference $\Delta\varpi$ librates around π . Outside S1, θ_2 and $\Delta\varpi$ alternate between libration and circulation, while in general θ_1 remains librating around zero until it reaches the domain formed by oscillations about Mode I. In this case, once again we have circulation of the critical angles. At the highest energy level (bottom panels in fig. 4), a separatrix (S2) appears inside the MMR domain, separating two distinct resonant regimes of motion. The new regime of motion (called RIV by Callegari *et al.*) fills the largest portions of the surfaces of section for higher energies (deep resonance). The dynamic power spectrum (at the right) shows that the lower frequency becomes equal to zero at the two points corresponding to the intersections of S2 with the x-axis. The direction of the phase flow inside the separatrix S2 is inverted with respect to what it is outside that separatrix. A true resonance occurs (with one proper frequency passing through zero). The dynamic power spectrum also shows that the solutions in the immediate neighborhood of S2 are chaotic. The above-discussed example (Callegari *et al.* 2004) is a true secular resonance inside the U-2N MMR \ddagger .

The appearance of the surface of section inside RIV is similar to that around MII, with only a different direction of the rotation. However, from the dynamical or topological point of view, these neighborhoods are very different. In the top panels, the apsidal proper frequency is always different from zero and the frequency variation from Mode II oscillations to circulations and to Mode I oscillations (from right to left in fig. 4*top.*) is smooth (continuous). In the bottom panels, the apsidal proper frequency is equal to zero at the separatrix S2; thus, the motions inside and outside S2 are separated by a true infinite-period separatrix (bifurcation) and no continuous transformation exist going across S2.

4. Mean-Motion Resonances and Apsidal Corotations

The surfaces of section in fig. 4 show that the anti-aligned periapses of the solutions in Mode II are preserved in the evolution of a system of two low-eccentricity planets towards resonance (notwithstanding the fact that the critical angles are circulating in Mode II and librating in RIII and RIV). The surfaces of section with energies intermediary between the two shown in fig. 4 (*top* and *middle*) show that the separatrix S1 emanates from the very position of the periodic orbit labeled MII in the secular dynamics and increases up to encompass the whole domain of solutions about $\Delta\varpi = \pi$ and even large amplitude oscillations around $\Delta\varpi = 0$ (see Callegari *et al.* 2004). This is a situation completely different of that occurring in the capture of a particle into a resonance with one planet (or satellite). In that case, the only effect is the capture of the critical angle \ddagger

$$\theta_1 = (p + q)\lambda' - p\lambda - q\varpi$$

about 0 or π . The sidereal periods of particle and planet become approximately commensurable but the pericenter of the particle orbit (whose longitude is ϖ) continues to rotate. That is, $\Delta\varpi = \varpi - \varpi'$ has a monotonic time variation. However, for some well defined values of the eccentricity of the planet (satellite) orbit, it happens that not only the angle θ_1 but also the angle

$$\theta_2 = (p + q)\lambda' - p\lambda - q\varpi'$$

\ddagger Other examples of true secular resonance were given by Michtchenko and Ferraz-Mello (2001b) and Michtchenko and Malhotra (2004).

\ddagger λ and ϖ are the mean longitude and longitude of the periapsis of the trapped particle, respectively, and λ' and ϖ' are those of the trapping planet (or satellite).

is trapped in the neighborhood of 0 or π . Consequently, $\Delta\varpi$ is no longer circulating but librating (Ferraz-Mello *et al.* 1993). This is the same phenomenon known as corotation resonance in disc and ring dynamics (motion following the resonance pattern speed), extended to beyond the narrow 1:1 resonance case of the epicyclic orbits theory. The characterization of corotation resonance given by Greenberg and Brahic (1984): “resonance that depends on the eccentricity of the perturbing satellite, rather than on the eccentricity of the perturbed particle” means that we have a corotation resonance when θ_2 is in libration. But, in the trapping particle problem, θ_2 cannot be in libration if θ_1 is circulating. Therefore the simultaneous libration of $\Delta\varpi$ and θ_1 is synonymous of resonance corotation.

The resonant planar planetary three-body problem (averaged over short-period terms) is a two-degree of freedom system (see Beaugé *et al.* 2003). “Exact apsidal corotations” are solutions for which the angles

$$\begin{aligned}\theta_1 &= (p+q)\lambda_2 - p\lambda_1 - q\varpi_1 \\ \theta_2 &= (p+q)\lambda_2 - p\lambda_1 - q\varpi_2.\end{aligned}$$

and the momenta I_1, I_2 conjugated to them remain constant in time. It is important to notice that these equilibrium solutions of the averaged equations correspond to periodic orbits of the non-averaged problem. Initial conditions close to them are periodic solutions of the averaged equations (quasi-periodic solutions of the non-averaged problem): oscillations around the fixed point of the averaged system. One such solution with finite amplitude oscillations will be generically referred to as “apsidal corotation resonance”, or, for short, “apsidal corotation”.

Although apsidal corotations have gained certain notoriety in exoplanetary dynamics, they are not new and can be found in our own Solar System. It has long been known (see Greenberg 1987 and references therein) that the Io-Europa pair is trapped in a 2/1 MMR and is in apsidal corotation. Both θ_1 and $\Delta\varpi$ oscillate (with very small amplitude) around fixed values. The exact apsidal corotation is defined in this case by $\theta_1 = 0$ and $\Delta\varpi = \pi$. We will refer to this case as a $(0, \pi)$ -corotation, a denomination more accurate than just saying that the apsides are *anti-aligned*.

GJ 876, the first extra-solar resonant planetary system ever discovered around a main-sequence star, also exhibits an apsidal corotation, although in this case the angular variables oscillate around $\theta_1 = 0$ and $\Delta\varpi = 0$. We will denote this as an $(0, 0)$ -corotation (the apsides are *aligned*).

The difference in behavior in these corotations is associated with the eccentricities of these solutions (see Lee and Peale, 2002; Beaugé *et al.* 2003): The $(0, \pi)$ solutions occur for low eccentricities of the bodies, while $(0, 0)$ corotations occur for larger eccentricities. Until recently there was little information about the exact border between both modes. The first study of families of periodic solutions of the exact equations of planets in 2/1 MMR, considering different eccentricities but constant planetary masses, is due to Hadjidemetriou (2002). Via numerical continuation of initially circular orbits for planetary masses similar to GJ 876, Hadjidemetriou (2002) found that the $(0, \pi)$ and $(0, 0)$ families are actually linked at $(e_1, e_2) = (0.097, 0)$, and it is possible to pass from one to another by a smooth variation of the total angular momentum.

Later discoveries of other extra-solar candidates in the same commensurability (as HD82943) also showed the system in apsidal corotation. The same seems to be true in other cases as the published orbits of two of the 55 Cnc planets, which lie in the 3/1 MMR. Even though some orbital fits are very imprecise, they seem to indicate that apsidal corotation resonance constitutes strong stabilizing mechanisms for high-eccentricity

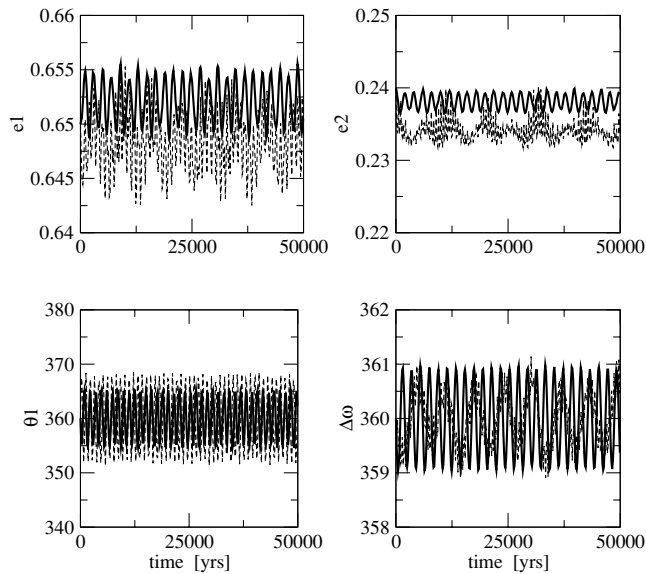


Figure 5. Two solutions in $(0, 0)$ apsidal corotation. Solid lines correspond to the masses and initial conditions given in Table 4. Dashed lines are solutions obtained with same initial eccentricities and angular variables, but increasing both the masses and semi-major axes by a factor 10.

resonant planets orbiting close to the central star. These examples justify the significant effort done in recent years to study the location and stability of all apsidal corotations allowing all families of corotations to be determined as function of the planets masses and orbital elements.

Systematic searches using averaged analytical models and numerical simulations with adiabatic migration were undertaken by Beaugé *et al.* (2003) and Ferraz-Mello *et al.* (2003) aiming at finding all possible stable apsidal corotations in the 2:1 and 3:1 MMR, as functions of all the parameters of the system. The first results were that, up to second order of the masses, the position of corotations is only a function of the mass ratio m_2/m_1 of the planets, not depending on the individual masses themselves (as long as they are not large).

Similarly, the solutions are practically independent of the semi-major axes a_1, a_2 , but only vary according to the value of the ratio $\alpha = a_1/a_2$. These facts are illustrated in figure 5 where solid lines correspond to a numerical simulation of a $(0, 0)$ -corotation (using initial conditions shown in Table 4) while dashed lines show results obtained with the same initial conditions, but increasing the planetary masses and semi-major axes by a factor 10. Although the oscillations around the exact apsidal corotation have different periods (see Beaugé *et al.* 2004), the overall behavior is practically the same. This makes clear that solutions found for given values of the six-parameter set $(m_2/m_1, \alpha, e_1, e_2, \theta_1, \Delta\varpi)$ should be valid for any resonant exoplanetary system, independent of their proximity to the star or size of the bodies.

Another important result of these investigation was the discovery of a different mode of apsidal corotation, where the equilibrium values of the angles are not equal to zero or π . They were found in both the 2/1 and 3/1 MMR and we called them “asymmetric corotations”. The published orbits of the inner planets of 55Cnc seem to correspond to such an asymmetric configuration (Beaugé *et al.* 2003, Zhou *et al.* 2004).

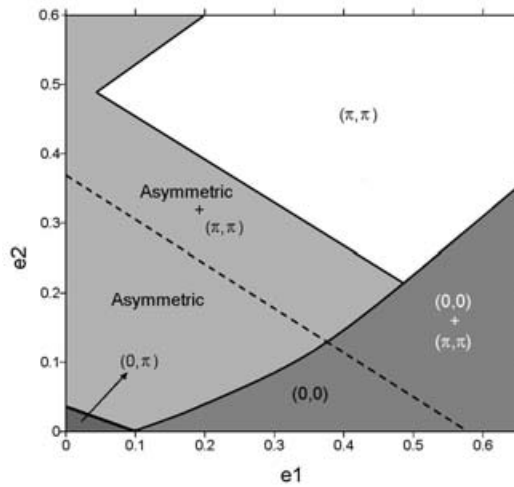


Figure 6. Domains of different types of exact apsidal corotations in the 2/1 mean-motion resonance in the e_1, e_2 -plane. See text for details.

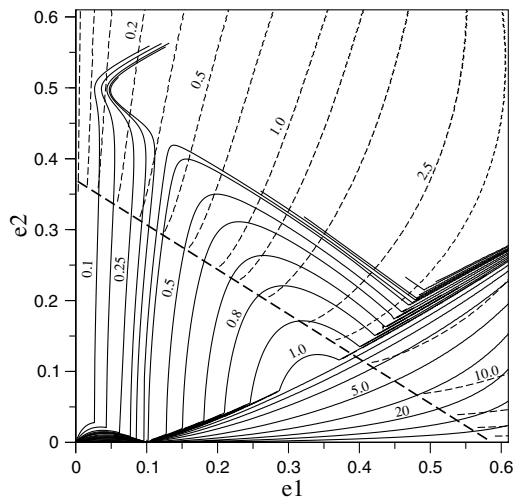


Figure 7. Level curves of constant mass ratio (i.e. $m_2/m_1 = \text{const.}$) in the eccentricity plane for the 2/1 MMR. Broken curves show the (π, π) corotations.

However, the diversity of apsidal corotations does not stop here. Numerical studies by Hadjidemetriou and Psychoyos (2003) and by Ji *et al.* (2003) have shown a new type of solutions at very high eccentricities. Although they are symmetric, they correspond to equilibrium values $\theta_1 = \pi$, $\Delta\varpi = \pi$. We have called them (π, π) -corotations. The orbital elements initially published for HD82943 (Geneva planet search web page, July 31th, 2002) seemed to correspond to such a configuration.

Lee (2004) used numerical simulations with differential migration to map the extent of this new family, finding that stable solutions are located beyond the line defined by the collision condition of the (π, π) corotations: $a_1(1 + e_1) = a_2(1 - e_2)$. This theoretical boundary is a limit for planet masses tending to zero. In fact, averaged models are not valid if the two planets come very close one to another, the minimal distance allowed

being proportional to the cube root of the planet masses (see Gladman, 1993). A similar task was also undertaken by Beaugé *et al.* (2004) with a semi-analytical method.

The main results for the 2/1 resonance are seen in Figure 6, which shows the limits of the domains of all types of apsidal corotation in the (e_1, e_2) -plane. One may also note that the (π, π) -corotations domain covers a large area at very high eccentricities; some parts of this domain overlaps with the asymmetric region, as well as the domain of $(0, 0)$ -corotations, for smaller values of e_2 . In the overlapping area, two distinct types of stable solutions coexist, in some cases even for the same values of the mass ratios.

Numerical simulations by Ferraz-Mello *et al.* (2003) and Lee (2004) have shown that $(0, 0)$, $(0, \pi)$ and asymmetric apsidal corotations are linked by isopleths of equal mass ratio m_2/m_1 (see fig. 7). Every solution corresponds to a well-defined value of the mass ratio and, depending on the value of this ratio, a given exoplanetary system may exhibit different types of corotations. All exact apsidal corotations in these families can be reached by constant mass-ratio paths starting from initially circular orbits. This is not the case of the (π, π) apsidal corotations, which do not appear to be reachable via a smooth variation of the parameters from a path starting from the low-eccentricity domains. Even in the domain where $(0, 0)$ and (π, π) overlap it does not seem possible to have a smooth change of one into another.

Figures 8 and 9 show concrete examples of different solutions of this problem. In all cases, we can see a very stable motion around one exact apsidal corotations with a relatively small amplitude of oscillation.

Figure 8 shows two asymmetric solutions. As pointed by Lee (2004), if the mass ratio satisfies the condition $m_2/m_1 > 0.4$, the asymmetric family returns to the $(0, 0)$ region for large values of e_1 . Conversely, if the mass ratio is smaller than this value, the asymmetric corotations seem to converge to a thin diagonal region for large values of e_2 . The two numerical simulations shown in this figure correspond to each case. In gray we can see an example of the upper high-eccentricity domain, while in black we present an asymmetric corotation in the main domain.

Figure 9 shows examples of the $(0, 0)$ and (π, π) cases taken in the rightmost area where both solutions are possible. The two orbits shown have the same planetary masses and same initial semi-major axes and eccentricities. Only the angles are different showing that both apparently opposite behaviors are possible. We point out that, in the two cases, the eccentricities do not have exactly the same averaged value (although very similar) due to the different initial phase angles chosen in each case.

The examples shown in figs. 5, 8 and 9 were obtained with numerical integrations of the exact equations with the masses and initial elements shown in Table 4.

5. Planetary Migration

Although apsidal corotation is a necessary condition for the survival of massive planets in nearby high-eccentricity orbits, they are nevertheless very particular solutions of the planetary three-body problem. The fact that they are verified by some exoplanetary systems raises interesting questions about their origin: Were the planets formed in such orbits? Or did they evolve towards them?

From early statistical studies by Roy and Ovenden (1954), it is known that it is highly improbable to find two massive bodies in an exact mean-motion resonance if they were formed independently. For instance, in the outer Solar System, the existence of several pairs of resonant satellites can only be explained by a past smooth variation of their semi-major axes due to tidal interactions; in other words, the current configuration is due to a “migration” of the primordial non-resonant orbits until a *resonance trapping* took place.

	$(0, \pi)$	Asym	U.Asym	$(0, 0)$	(π, π)
m_1	1.0	1.0	1.0	1.0	1.0
m_2	0.016	0.607	0.0136	5.5	5.5
a_1	0.6295	0.6291	0.6295	0.6295	0.6295
a_2	1.0	1.0	1.0	1.0	1.0
e_1	0.03	0.20	0.13	0.65	0.65
e_2	0.02	0.28	0.57	0.24	0.24
λ_1	0.0	36.92	178.4	0.0	180.0
λ_2	0.0	216.92	358.4	180.0	180.0
ϖ_1	0.0	0.0	0.0	0.0	0.0
ϖ_2	180.0	97.17	264.14	0.0	180.0

Table 4. Initial conditions of the small amplitude corotations shown in figs. 5, 8 and 9. “Asym” = Main domain of asymmetric corotations; “U.Asym” = Upper domain of Asymmetric corotations. Planetary masses are in units of $10^{-4}M_{\odot}$. The mass of the central star is taken as $1M_{\odot}$

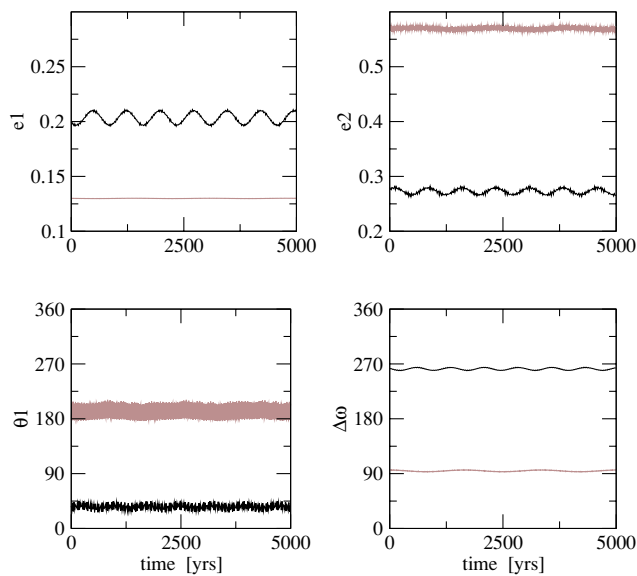


Figure 8. Numerical simulation of two initial conditions in asymmetric corotation. Black shows an example of the low-eccentricity region, while in gray we present a case of the Upper asymmetric domain. Initial conditions are given in Table 4.

After the trapping, both satellites remained locked in stable orbits with commensurable periods. If migration continued after the trapping, both bodies evolved in such a way as to maintain the resonance relationship intact. To say that a similar scenario occurred in exoplanets depends on two things: (i) to find a plausible driving mechanism for planetary migration, compatible with the formation process of the system, and (ii) to prove that this orbital evolution allows resonance capture, and yields final orbits in apsidal corotation.

In the past few years, several works have undertaken these questions. Although several migration mechanism have been initially proposed, it seems that the most probable process stems from the interaction between the planets and the gaseous primordial disk. Hydrodynamical simulations by Kley (2001, 2003), Snellgrove *et al.* (2001) and Papaloizou (2003), among others, have shown that an adequate choice of the

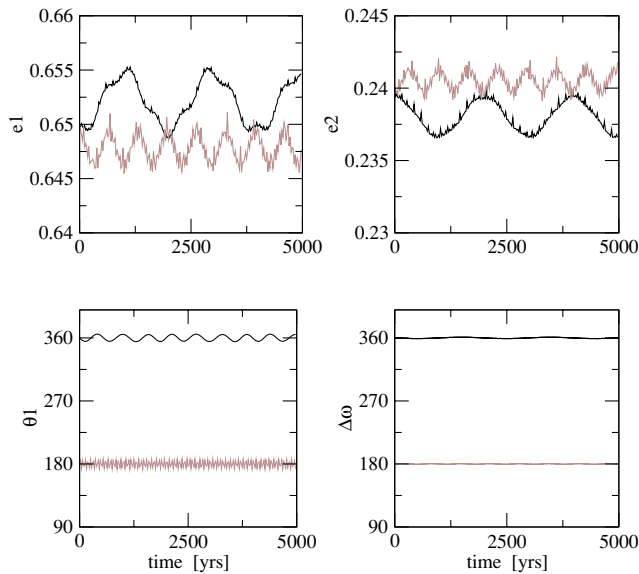


Figure 9. Numerical integration of two orbits with the same masses, semi-major axes and eccentricities. The initial angular variables were varied to place them in a stable $(0, 0)$ and (π, π) -corotation. Initial conditions are given in Table 4.

parameters of the gaseous disk can favor both, a large-scale inward migration and a resonance trapping in corotation.

However, not all apsidal corotations can result from this scenario. In the case of the $2/1$ resonance, we can group the different families into two distinct classes:

- Type I. Families that can be obtained through analytical continuation from initial circular orbits $e_1 = e_2 = 0$. It includes the $(0, \pi)$, $(0, 0)$ and the asymmetrical families.
- Type II. The (π, π) solutions. At variance with the previous ones, this kinds of apsidal corotation does not appear to be reachable via a smooth variation of the parameters from the low-eccentricity domains.

From the point of view of migration, only Type I corotations can be attained through a smooth orbital evolution starting from quasi-circular orbits. Thus, if the planetary migration hypothesis is correct, and if all exoplanets entered the mean-motion resonance in quasi-circular orbits, then we should only expect to observe Type I solutions in real systems. The extra-solar planetary systems presently confirmed in the $2/1$ resonance, GJ 876 and HD82843, show Type I apsidal corotations. In the $3/1$ resonance, the published orbit of 55 Cnc also corresponds to a Type I apsidal corotation (Beaugé *et al.* 2003, Zhou *et al.* 2004).

In fact, there is only one system proposed to be in $2:1$ MMR and Type II corotation: the outer planets of HD160691 (Bois *et al.* 2003). However, more recent observations rule out the possibility of a $2:1$ MMR in this case (Goździewski *et al.* 2003, McCarthy, 2004). Anyway, a (π, π) apsidal corotation was unlikely, since no adiabatic evolutionary process could lead to such a situation.

6. Conclusions

In this review, we have presented a brief look at recent results on the dynamics of extra-solar planetary systems. We have separated the known planetary systems into four

main groups: (Ia) Planets in Mean-motion resonance (Ib) Low-eccentricity near-resonant pairs; (II) Non-resonant planets with a significant secular dynamics; and (III) Weakly interacting planet pairs. This division reflects the different degree of interaction between the planets and, consequently, the different analytical models necessary to study their evolution and stability.

Recently, the works of Callegari *et al.* (2004) and of Michtchenko and Malhotra (2004), on the dynamics of systems with a significant secular dynamics, have shown new types of motion, many of which unknown until very recently. The same can be said for MMR, where an increasingly complex structure has been discovered. Even such simple solutions as the exact apsidal corotations (which are simply fixed points of the averaged system) show a large diversity of behavior.

A more difficult question is whether each class of extra-solar planetary systems is indicative of different past evolutions and formation scenarios. Resonant pairs are strong evidence in favor of a large-scale planetary migration before the dispersal of the stellar nebula. However, it is not very clear how systems with small period ratio but not resonant fit into this picture. Future work on disk-planet interactions, as well as better models of capture into resonance and/or scattering will help us define more clearly the relation between present day dynamics and the planetary origin.

Acknowledgements

This work has been supported by the Argentinian Research Council – CONICET –, the Brazilian National Research Council – CNPq – and the São Paulo State Science Foundation – FAPESP.

References

- Beaugé, C., Ferraz-Mello, S. and Michtchenko, T.A. 2003, *Astrophys. J.*, 593, 1124
- Beaugé, C., Ferraz-Mello, S. and Michtchenko, T.A. 2004, *Mon. Not. R. Astron. Soc.*, submitted (astro-ph/0404166)
- Bois, E., Kiseleva-Eggleton, L., Rambaux, N. and Pilat-Lohinger, E. 2003, *Astrophys. J.*, 598, 1312
- Callegari Jr., N., Michtchenko, T. and Ferraz-Mello, S. 2004, *Cel. Mech. Dyn. Astron.* 89, 201
- Ferraz-Mello, S., Tsuchida, M. and Klafke, J.C. 1993, *Cel. Mech. Dyn. Astron.*, 55, 25
- Ferraz-Mello, S. and Michtchenko, T.A. 2003, *Rev. Mexic. Astr. Astrof. (serie conf.)*, 14, 7
- Ferraz-Mello, S., Beaugé, C. and Michtchenko, T.A. 2003, *Cel. Mech. Dyn. Astron.* 87, 99
- Ferraz-Mello, S., Michtchenko, T.A. and Beaugé, C. 2004, *Astrophys. J.*, in press
- Fischer, D.A., Marcy, G.W., Butler, R.P., Vogt, S.S., Henry, G.W., Pourbaix, D., Walp, B., Misch, A.A. and Wright, J.T. 2003, *Astrophys. J.* 586, 1394
- Gladman, B. 1993, *Icarus*, 106, 247
- Greenberg, R. and Brahic, A. (eds.) (1984). *Planetary Rings*, Univ. Arizona Press.
- Goździewski, K., Konacki, M. and Maciejewski, A.J. 2003, *Astrophys. J.* 594, 1019
- Greenberg, R. 1987, *Icarus*, 70, 334
- Hadjidemetriou, J. 2002, *Cel. Mech. Dyn. Astron.*, 83, 141
- Hadjidemetriou, J. and Psychoyos, D. 2003, in: G. Contopoulos and N. Voglis (eds.) *Galaxies and Chaos*, Lecture Notes in Physics. Springer-Verlag, p 412
- Ji, J., Liu, L., Kinoshita, H., Zhou, J., Nakai, H. and Li, G. 2003, *Astrophys. J.*, 591, L57
- Kley, W. 2001, *Mon. Not. R. Astron. Soc.*, 313, L47
- Kley, W. 2003, *Cel. Mech. Dyn. Astron.*, 87, 85
- Konacki, M. and Wolszczan, A. 2003, *Astrophys. J.* 591, L147
- Laskar, J. 1993, *Physica D*, 67, 257
- Lee, M.H. and Peale, S.J. 2002, *Astrophys. J.*, 567, 596
- Lee, M.H. and Peale, S.J. 2003, *Astrophys. J.*, 592, 1201

- Lee, M.H. 2004, *Astrophys. J.*, 611, 517
- McArthur, B.E., Endl, M., Cochran, W.D., Benedict, G.F., Fischer, D.A., Marcy, G.W., Butler, R.P., Naef, D., Mayor, M., Queloz, D., Udry, S. and Harrison, T.E. 2004, *Astrophys. J.* 614, L81
- McCarthy, C., Butler, R.P., Tinney, C.G., Jones, H.R.A., Marcy, G.W., Carter, B., Penny, A.J. and Fischer, D.A. 2004, *Astrophys. J.*, submitted (Astro-ph/0409335)
- Malhotra, R., Black, D., Eck, A. and Jackson, A. 1992, *Nature* 355, 583
- Michtchenko, T. A. and Ferraz-Mello, S. 2001a, *Astron. J.* 122, 474
- Michtchenko, T. A. and Ferraz-Mello, S. 2001b, *Icarus* 149, 357
- Michtchenko, T. and Malhotra, R. 2004, *Icarus*, 169, 237
- Naef, D., Mayor, M., Beuzit, J.L., Perrier, C., Queloz, D., Sivan, J.P. and Udry, S. 2004, *Astron. Astrophys.*, 414, 351
- Papaloizou, J.C.B. 2003, *Cel. Mech. Dyn. Astron.*, 87, 53
- Pauwels, T. 1983, *Celest. Mech.*, 30, 229
- Rasio, F.A., Nicholson, P.D., Shapiro, S.L. and Teukolsky, S.A. 1992, *Nature*, 355, 325
- Roy, A.E. and Ovenden, M.W. 1954, *Mon. Not. R. Astron. Soc.*, 114, 232
- Santos, N., Bouchy, F., Mayor, M., Pepe, F., Queloz, D., Udry, S., Lovis, C., Bazot, M., Benz, W., Bertaux, J.-L., LoCurto, G., Delfosse, X., Mordasini, C., Naef, D., Sivan, J.P. and Vauclair, S. 2004, *Astron. Astrophys.* (submitted)
- Schneider, J. 2004, *Extra-solar planets Encyclopaedia*, [http:// www.obspm.fr/ planets](http://www.obspm.fr/planets)
- Snellgrove, M.D., Papaloizou, J.C.B. and Nelson, R.P. 2001, *Astron. Astrophys.*, 374, 1092
- Zhou, L-Y., Lehto, H.J., Sun, Y-S. and Zheng, J-Q. 2004, *Mon. Not. R. Astron. Soc.* (submitted)